Long-Distance Correlations of Charged Particles*

M. WADATI AND A. ISIHARA
Statistical Physics Laboratory, Department of Physics and Astronomy, State University of New York, Buffalo, New York 14214
(Received 7 July 1969)

The spatial correlation functions of charged particles are evaluated explicitly in the chain-diagram approximation. The results are important at large distances. Three different cases are considered: (1) classical electrons, (2) metallic electrons, and (3) charged bosons. Quantum corrections to the correlation function of classical electrons is expressed in terms of a convenient parameter $\alpha=\lambda\kappa_0$, where λ is the de Broglie thermal wavelength and κ_0 is the Debye constant. The correlation function of metallic electrons deviates from that of classical electrons markedly for higher densities. It is evaluated for several different densities. The correlation functions of charged bosons for various densities can be reduced in a universal form. The fermion and boson cases are evaluated for 0°K. The resulting curves show small oscillations at relatively large distances.

1. INTRODUCTION

In recent articles we have derived formulas for the spatial correlation functions of systems of charged particles based on the chain-diagram approximation.[1] Our main interest in this approximation is in finding collective couplings of particles at large distances. In this paper we report explicit results obtained by numerical computations. The systems of our consideration include the following: (1) classical electron gas with quantum corrections, (2) metallic electrons at very low temperatures, and (3) charged bosons at very low temperatures. Furthermore, we discuss analytically quantum corrections to the correlation function of a classical electron gas. The corrections are important to remove short-distance divergence of the correlation function.

We follow our previous notations and express the pair distribution function by $\rho_2(r)$. We choose the units such that $\hbar=1$ and $2m=1$, where m is the particle mass.

2. CLASSICAL ELECTRON GAS WITH QUANTUM CORRECTIONS

The pair distribution function in the simple chain-diagram approximation for a classical electron gas is given by

$$\rho_2(r)/n^2-1=-\epsilon(e^{-x}/x), \tag{2.1}$$

where $\epsilon=\beta e^2\kappa_0$ is called the plasma parameter, $\kappa_0=(4\pi n\beta e^2)^{1/2}$ is the Debye constant, and x is the reduced distance defined by

$$x=\kappa_0 r. \tag{2.2}$$

Expression (2.1) is correct to first order in the plasma parameter. The correction to this result can be obtained by consideration of more complex diagrams.[2,3] Especially the short-distance divergence in this result can be removed by introducing watermelon-type diagrams. The result is[4]

$$\rho_2(r)=n^2\exp\left(-\epsilon(e^{-x}/x)\right). \tag{2.3}$$

The divergence does not exist when quantum statistics is introduced.[5] We shall discuss a new interpolation formula which improves the expression reported recently by Disendorf and Ninham[6] based on Montroll and Ward's method.[7] Their result is given by

$$\rho_2(r)/n^2-1=-(\tfrac{1}{2}\pi)^{1/2}(\epsilon/\alpha) \quad \text{for} \quad x\ll\alpha\ll1 \tag{2.4a}$$

$$=-(\epsilon/x)\{e^{-x}-2(\alpha/x)^2e^{-(1/2)(x/\alpha)^2}\} \quad \text{for} \quad x\gg\alpha, \tag{2.4b}$$

where λ is the thermal de Broglie wavelength which is in our units $\beta^{1/2}$ and

$$\alpha=\lambda\kappa_0. \tag{2.5}$$

By a somewhat different method we have obtained an interpolation formula which is valid for all distances. The result is

$$\rho_2(r)/n^2-1=-\epsilon\left\{\frac{e^{-x}}{x}-\frac{e^{-(1/2)(x/\alpha)^2}}{x}+\frac{2^{1/2}}{\alpha}\operatorname{erfc}\left(\frac{x}{2^{1/2}\alpha}\right)\right\}, \tag{2.6}$$

where

$$\operatorname{erfc}(x)=\int_x^\infty e^{-y^2}dy.$$

---

* This work was supported by the National Science Foundation. Part of this work was submitted by one of the authors (M. W.) to the State University of New York in partial fulfillment of the requirements of a Ph.D. degree. It was completed while the other author was visiting the Solid State Science Division of the Argonne National Laboratory under support of the U. S. Atomic Energy Commission.

[1] A. Isihara and M. Wadati, Phys. Rev. **183**, 312 (1969).

[2] D. L. Bowers and E. E. Salpeter, Phys. Rev. **119**, 1180 (1960).

[3] A. Isihara, Phys. Rev. **178**, 412 (1969).

[4] Results based on Monte Carlo calculations have been shown to agree with Eq. (2.3). See S. G. Brush, H. L. Sahlin, and E. Teller, J. Chem. Phys. **45**, 2102 (1966).

[5] The importance of quantum corrections at short distances has been discussed by several authors. See, for example, T. Morita, Progr. Theoret. Phys. (Kyoto) **22**, 757 (1959); B. A. Trubnikov and V. F. Elsin, Zh. Eksperim. i Teor. Fiz **47**, 1279 (1964) [English transl.: Soviet Phys.—JETP **20**, 866 (1965)].

[6] M. Disendorf and B. W. Ninham, J. Math. Phys. **9**, 745 (1968); referred to hereafter as DN.

[7] E. W. Montroll and J. C. Ward, Phys. Fluids **1**, 55 (1958).

In the limits Eq. (2.6) yields the DN results of Eqs. (2.4). In fact, for $x\ll\alpha\ll 1$ it gives

$$\rho_2(r)/n^2=1-(\tfrac{1}{2}\pi)^{1/2}(\epsilon/\alpha)+(\epsilon/2\alpha^2)x. \tag{2.7}$$

Before deriving our formula (2.6) let us compare the pair distribution functions based on the above formulas numerically. Curves I, II, and III in Figs. 1 and 2 represent, respectively, Eqs. (2.1), (2.3), and (2.6). Figure 1 corresponds to $\epsilon=0.001$ and Fig. 2 to $\epsilon=0.0005$. Thus, quantum corrections are more effective in Fig. 1 than in Fig. 2. Note in both cases curves III are finite at the origin and approach I at large distances. The ordinate of III at the origin depends on the plasma parameter ϵ and α.

Curves I in Figs. 1 and 2 start showing the short distance divergence at around $x=2\times 10^{-3}$. In the classical limit both $\lambda\!\!\!^{-}$ and α approach zero, and Eq. (2.6) reduces itself to Eq. (2.3).

The ϵ values 0.001 and 0.0005 in Figs. 1 and 2 give curve III below and above curve II near the origin. One could bring curve III to the origin by choosing ϵ somewhere between the two values.

We now discuss the derivation of Eq. (2.6). The deviation of the pair distribution function from an ideal quantum gas term is given by

$$\Delta\rho_2(r)-n^2=-\frac{4}{(2\pi)^3\beta}\sum_j\int\frac{\lambda_j^2u(q)}{1+2\lambda_ju(q)}e^{-i\mathbf{q}\cdot\mathbf{r}}d\mathbf{q}, \tag{2.8}$$

where

$$\begin{aligned}&u(q)=4\pi e^2/q^2,\\ &\lambda_j(q)=z\lambda^{-3}\int_0^\beta e^{-q^2(\alpha/\beta)(\beta-\alpha)}e^{2\pi ij(\alpha/\beta)}d\alpha.\end{aligned} \tag{2.9}$$

z is the absolute activity.

At high temperature and low density the Debye length κ_0^{-1} is much larger than de Broglie wavelength $\lambda\!\!\!^{-}$. For $r\gg\lambda\!\!\!^{-}$ the Debye approximation results in from the above formula (2.8) because the eigenvalues can be expanded in powers of βq^2 as follows:

$$\lambda_j(q)=(z\beta/\lambda^3)\delta_{j0},\quad q\ll\beta^{-1/2}. \tag{2.10}$$

To find a valid expression for $r\ll\kappa_0^{-1}$ we note that the main contribution to the integral of Eq. (2.8) comes from the domain of $\mathbf{q}$ satisfying

$$\lambda_j(q)u(q)\ll 1,\quad q\gg\kappa_0. \tag{2.11}$$

The two asymptotic results obtained from small and large q regions defined by (2.10) and (2.11) overlap in the intermediate region. We can obtain a satisfactory interpolation formula by evaluating the $\mathbf{q}$ integrations as follows:

$$\begin{aligned}\Delta\rho_2(r)-n^2=&-\frac{4}{(2\pi)^3\beta}\int_{q\le q_0}\frac{\lambda_0^2u}{1+2\lambda_0u}e^{i\mathbf{q}\cdot\mathbf{r}}d\mathbf{q}\\ &-\frac{4}{(2\pi)^3\beta}\sum_j\int_{q\ge q_0}\lambda_j^2ue^{i\mathbf{q}\cdot\mathbf{r}}d\mathbf{q},\end{aligned} \tag{2.12}$$

where q_0 is a certain momentum variable to be chosen between κ_0 and $\beta^{-1/2}$.

The first integral in Eq. (2.12) yields

$$2\pi\frac{z\beta}{\lambda^3}\kappa^2\left[\frac{1}{r}\frac{1}{2}\pi e^{-\kappa r}+\frac{1}{r}\,\mathrm{si}(q_0r)\right], \tag{2.13}$$

where

$$\begin{aligned}&\mathrm{si}(x)=-\int_x^\infty\frac{\sin t}{t}dt,\\ &\kappa^2=4\pi(2z/\lambda^3)\beta e^2.\end{aligned} \tag{2.14}$$

In the second integral we first perform the summation

$$\sum_j\lambda_j^2=\left(\frac{z\beta}{\lambda^3}\right)^2\int_0^1dx\int_0^1dy\,e^{-q^2x(1-x)\beta-q^2y(1-y)\beta}\times\sum_j e^{2\pi ij(x+y)}. \tag{2.15}$$

Using the relation

$$\sum_j e^{2\pi ij(x+y)}=\delta(x+y-m)$$

for integers m, we find

$$\begin{aligned}\sum_j\lambda_j^2&=\left(\frac{z\beta}{\lambda^3}\right)^2\int_0^1dx\,e^{-2q^2x(1-x)\beta}\\ &=\left(\frac{z\beta}{\lambda^3}\right)^2\frac{e^{-\beta q^2/2}}{(\beta q^2/2)^{1/2}}\int_0^{(\beta q^2/2)^{1/2}}e^{t^2}dt.\end{aligned} \tag{2.16}$$

The right-hand-side integral can be converged into an infinite integral by making use of the formula

$$\int_0^\infty e^{-q^2x^2}\sin bx\,dx=\frac{e^{-b^2/4a^2}}{a}\int_0^{b/2a}e^{t^2}dt. \tag{2.17}$$

After lengthy but straightforward calculations, we arrive at

$$2\pi\frac{z\beta}{\lambda^3}\kappa^2\left\{\frac{\pi}{2r}(-e^{-r^2/2\beta}+1)+\tfrac{1}{2}\pi\left(\frac{2}{\beta}\right)^{1/2}\times\mathrm{erfc}\left(\frac{r}{(2\beta)^{1/2}}\right)-\frac{1}{r}\,\mathrm{Si}(q_0r)\right\}, \tag{2.18}$$

where

$$\begin{aligned}&\mathrm{erfc}(x)=\int_x^\infty e^{-t^2}dt,\\ &\mathrm{Si}(x)=\int_0^x\frac{\sin t}{t}dt=\mathrm{si}(x)+\tfrac{1}{2}\pi.\end{aligned} \tag{2.19}$$

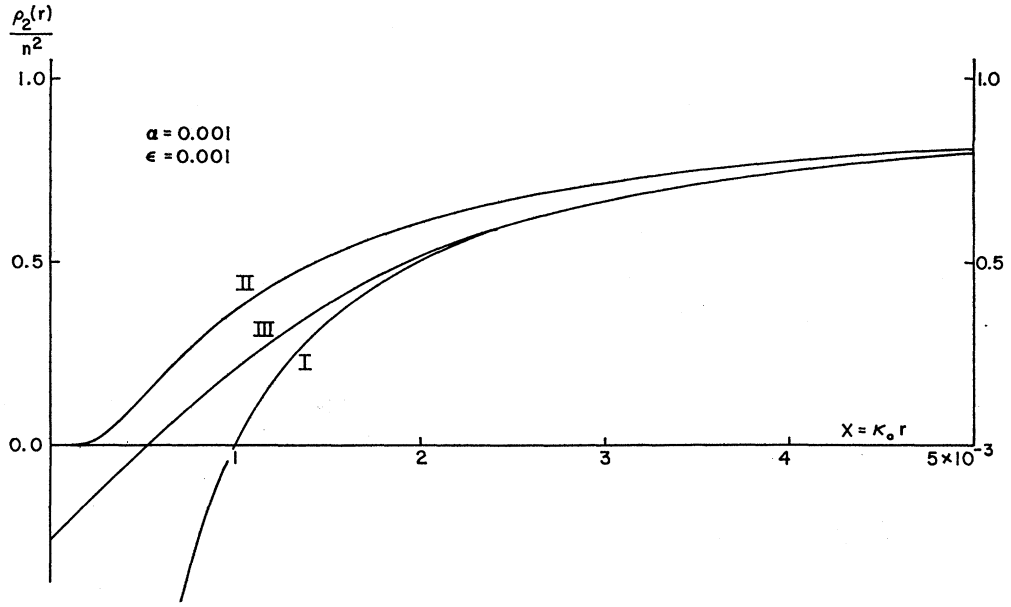

FIG. 1. Chain-diagram contribution to the pair distribution function of the classical electron gas for which $\epsilon=0.001$. x represents a reduced distance.

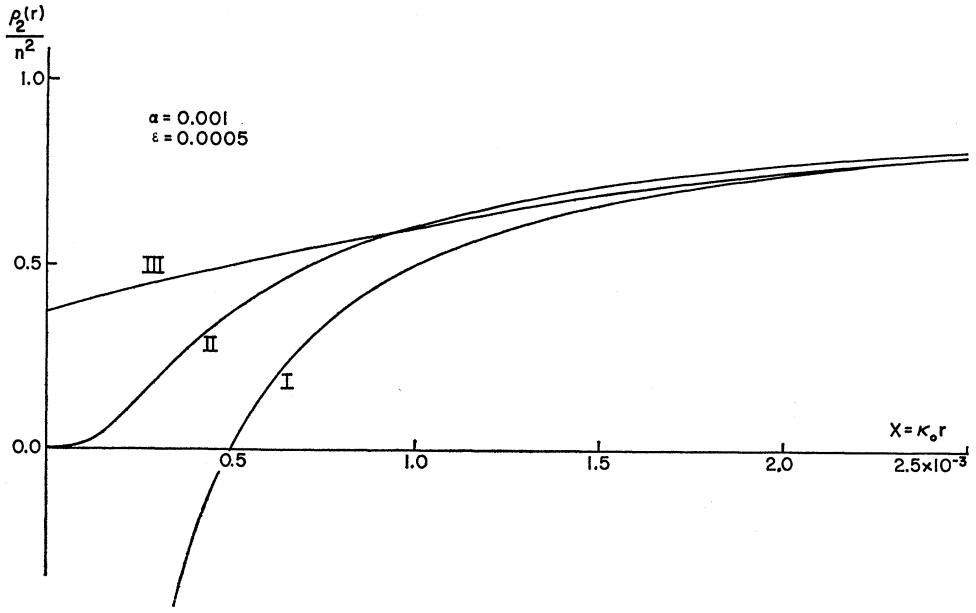

FIG. 2. Chain-diagram contribution to the pair distribution function of classical electrons ($\epsilon=0.0005$).

Summing the two integrals we obtain

$$\Delta\rho_2(r)-n^2=-\frac{2z}{\lambda^3}\kappa^2\left\{\frac{e^{-\kappa r}}{4\pi r}-\frac{e^{-r^2/2\beta}}{4\pi r}+\frac{1}{4\pi}\left(\frac{2}{\beta}\right)^{1/2}\operatorname{erfc}\left(\frac{r}{(2\beta)^{1/2}}\right)\right\}, \quad (2.20)$$

which is Eq. (2.6).

3. DEGENERATE ELECTRONS

The pair-distribution function for degenerate electrons at the lowest temperature in the chain-diagram approximation assumes the form for large distances

$$\frac{\Delta\rho_2(r)}{n^2}-1=-\frac{3}{2\pi^2}\left(\frac{3}{2\pi}\right)^{1/3}\frac{1}{r_s}\frac{1}{x}\times\int_0^\infty dy\int_0^\infty ds\frac{sF^2(s,y)\sin sx}{s^2+s_0^2F(s,y)}, \quad (3.1)$$

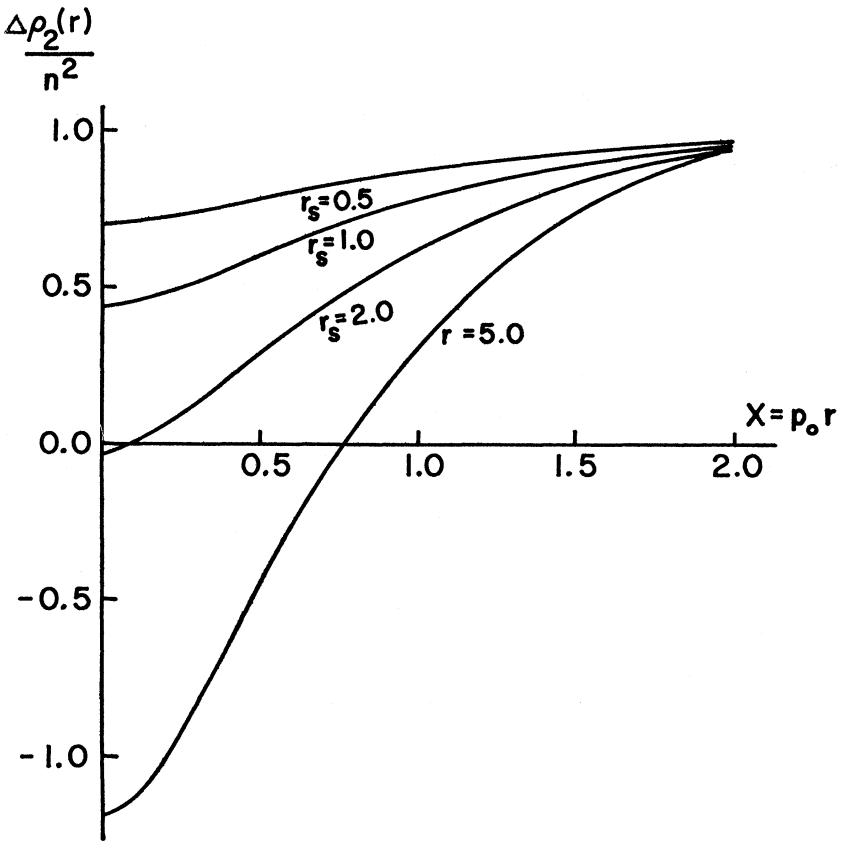

FIG. 3. Chain-diagram contribution to the pair distribution function of degenerated electrons at 0°K at short distances.

where

$$F(s,y)=1-\frac{1}{8}\left(s-\frac{4}{s}-\frac{y^2}{s^3}\right)\ln\frac{(s^2+2s)^2+y^2}{(s^2-2s)^2+y^2}$$
$$-\frac{y}{2s}\left\{\tan^{-1}\left(\frac{s^2+2s}{y}\right)-\tan^{-1}\left(\frac{s^2-2s}{y}\right)\right\}, \quad (3.2)$$

and

$$s=q/p_0, \quad x=p_0r, \quad p_0=(3\pi^2n)^{1/3},$$
$$s_0^2=\frac{2}{a_0p_0\pi}=0.331722r_s \quad \text{and} \quad r_s=(1/\tfrac{4}{3}\pi a_0^3n)^{1/3}. \quad (3.3)$$

r_s is the radius of the sphere which an electron occupies, measured by the Bohr radius. s and x are reduced momentum and distance variables, respectively.

We have evaluated the double integrals of Eq. (3.1) numerically for various values of r_s. The integrations over the variables y and s were carried from 0 to 50 after observing that widening the domains did not change the integrals much.

Figures 3 and 4 illustrate our results, where the former is for short distances and the latter is for large distances. It is interesting to observe that the pair distribution function becomes negative for metallic densities such as corresponding to $r_s=2.0$ and $r_s=5.0$. This is in agreement with what Glick and Ferrell observed[8] based on a different approach. The curve corresponding to $r_s=5.0$ increases very rapidly and becomes positive. This is a kind of Friedel oscillations in a much smaller scale. It should be remarked that such oscillations appear for very dilute cases and are enhanced if the random-phase approximation (RPA) is introduced.

The pair distribution function has been approximately evaluated by replacing the y integration by a single term corresponding to $y=0$.[9] Although this term is the largest, other small y terms give rise to non-negligible contributions. Because of the neglect of these terms and since the oscillations are more effective for dilute cases, the effective roles played by such oscillations in metals should be viewed with reservations. The stronger oscillations at lower densities can be seen in the well-known Langer and Vosko results based on the RPA.[9]

As the density increases r_s gets smaller and the maximum momentum p_0 becomes larger. Thus, we expect that the probability of finding a pair of fermions near the origin becomes larger for smaller r_s. In other words, the potential effects become smaller. This observation explains the tendency in Fig. 3.

[8] A. J. Glick and R. A. Ferrell, Ann. Phys. (N.Y.) 11, 359 (1960).
[9] J. Langer and S. J. Vosko, Phys. Chem. Solids 12, 196 (1960).

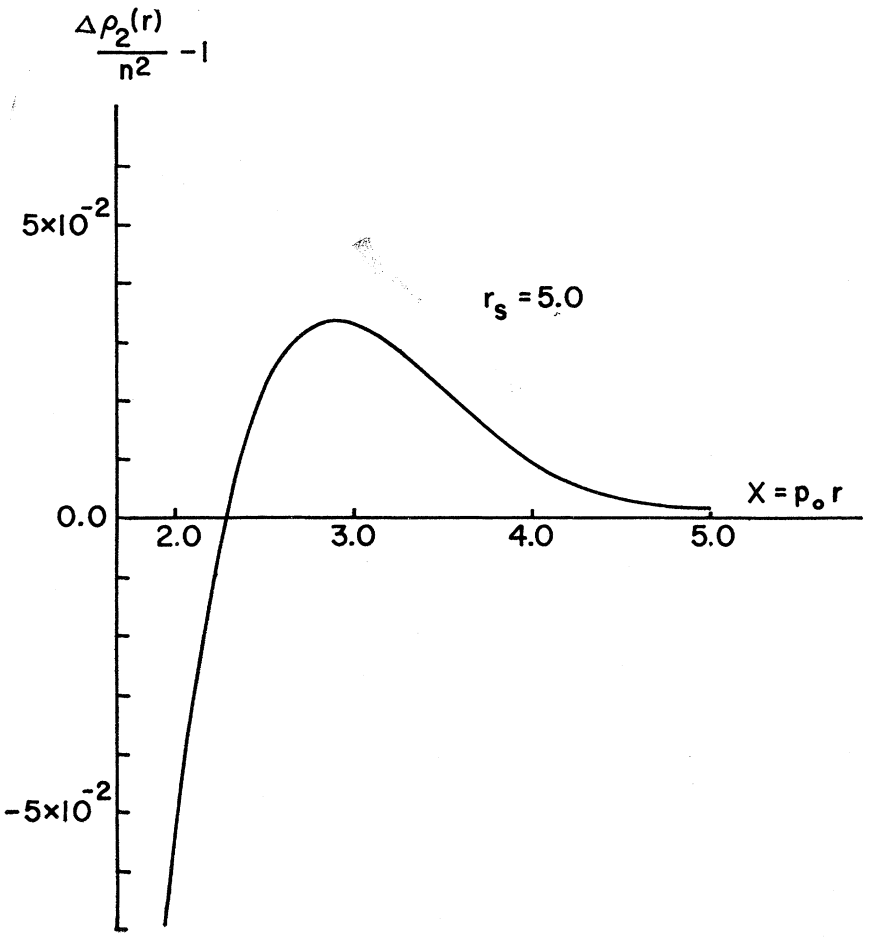

FIG. 4. Fermion pair distribution function corresponding to $r_s = 5.0$ of Fig. 3 in a large scale.

It has been discussed[10] that the negativeness at the origin in the pair distribution function evaluated in the RPA is due to the inapplicability of the approximation to such a density ($r_s \gtrsim 2.0$). This problem can be solved by taking other types of graphs into consideration. As we have discussed elsewhere,[11] for spinless cases ex-

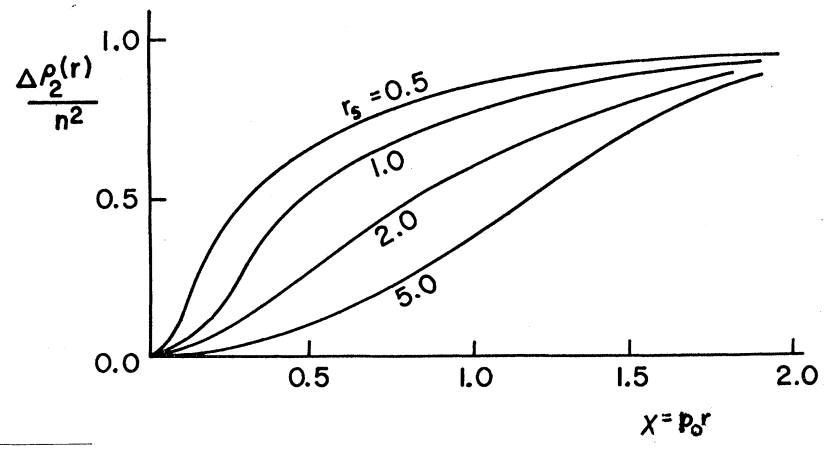

FIG. 5. Schematical curves illustrating Eq. (3.4) for various r_s values.

[10] D. Pines, *The Many Body Problem* (W. A. Benjamin, Inc., New York, 1962).
[11] A. Isihara, Phys. Rev. **172**, 166 (1968); J. Phys. Soc. Japan Suppl. **26**, 256 (1969).

change diagrams play important roles at short distances. Indeed, Eq. (2.8) should be replaced by

$$\Delta\rho_2(r)-n^2=-\frac{4}{(2\pi)^3\beta}\sum_j\int\left(\frac{u(q)}{1+\lambda_j u(q)}\right)\times[\lambda_j^2 e^{-iq\cdot r}-\lambda_j^2(q,r,z)]dq, \quad (3.4)$$

where the $\lambda_j(q,r,z)$ are the eigenvalues corresponding to exchange chain diagrams and satisfy $[\lambda_j(q,r,z)]_{r=0}=\lambda_j$. Equation (3.4) is schematically illustrated in Fig. 5.

4. CHARGED BOSONS

A system of bosons with Coulomb interactions may be considered as an idealized model for superconductive electrons. The pair distribution function for charged bosons at 0°K is given by

$$\frac{\Delta\rho_2(r)}{n^2}-1=-\frac{4}{\pi}\frac{2^{1/2}}{3^{1/4}}r_s^{3/4}\frac{1}{x}\times\int_0^\infty dy\, y^3\sin xy\left(\frac{1}{y^2}-\frac{1}{(y^4+1)^{1/2}}\right), \quad (4.1)$$

where $r_s=(1/\frac{4}{3}\pi a_0^3 n)^{1/3}$ as before, and

$$x=Ar, \quad A^4\equiv 8\pi n e^2. \quad (4.2)$$

Again, x represents a reduced-distance variable. Note that the reducing unit A^{-1} differs from the cases of classical and quantal electrons.

The asymptotic behavior of the pair distribution function is obtained from Eq. (4.1) as follows:

$$\frac{\Delta\rho_2(r)}{n^2}-1=-\frac{2^{1/2}}{3^{1/4}}r_s^{3/4}e^{-bx}\{b\cos bx+d\sin bx\}, \quad (4.3)$$

where the two characteristic constants b and d are just numbers given by

$$b^2=\tfrac{1}{2}(\sqrt{2}-1), \quad d^2=\tfrac{1}{2}(\sqrt{2}+1). \quad (4.4)$$

We have performed numerical evaluations based on Eq. (4.3). The short-distance behavior of the pair distribution function of charged bosons is illustrated in Fig. 6 for various r_s values. It should be remarked that in this case $(\rho_2(r)/n^2-1)r_s^{-3/4}$ is a universal function of the reduced distance x. Again, the pair distribution

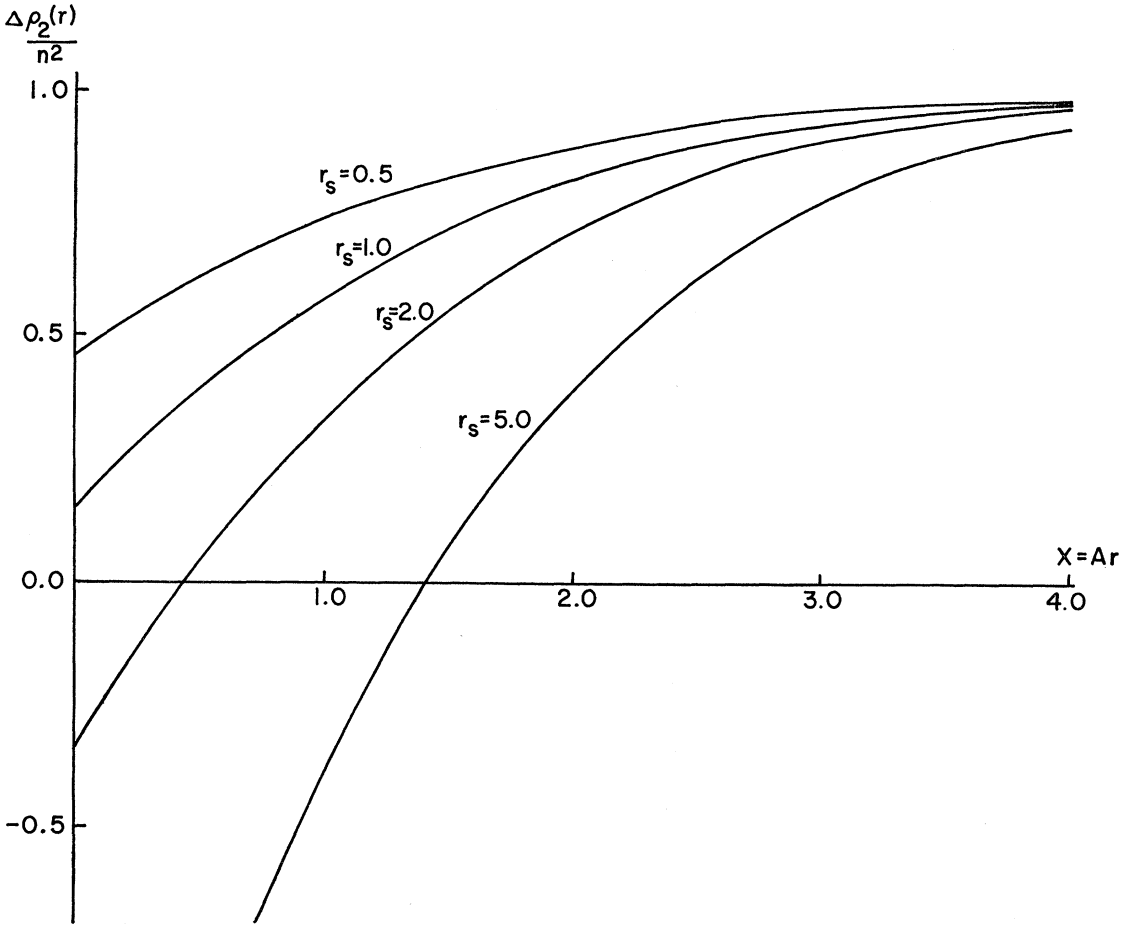

FIG. 6. Chain-diagram contribution to the pair distribution function of charged bosons at 0°K.

function becomes negative at short distances for $r_s \gtrsim 2.0$. Actually, in the case of bosons the ideal gas contribution to the pair distribution function is very large at short distances. In fact, $\rho_2(r)/n^2$ of an ideal Bose gas reaches 2.0 at $r=0$. Therefore, the total pair distribution function will look different from the case of fermions.

The large-distance behavior of the distribution function is illustrated in Fig. 7. After reaching a maximum, the correlation function starts oscillating at large distances in conformity with Eq. (4.4). In this range the correlation function is not of a screened Coulomb type but a simple exponential function with oscillating terms. The Coulomb repulsion tends to depress $\rho_2(r)$, while the statistics acts against, resulting in the oscillation. The oscillation is very slow in the reduced variable x, but it is there.

5. CONCLUDING REMARKS

We have seen the three different systems of charged particles. It should be remarked that in all cases we have evaluated the correlation functions in the chain-diagram approximation. This statement refers not only to the nature of our approximations but also to our results representing the contributions from interactions. The entire pair-distribution function is obtained by adding the contributions from noninteracting particles. However, such contributions are not very important at large distances as they decay rather fast. The pair distribution function of an ideal fermion gas is zero at $r=0$. Therefore, the curves in Fig. 3 will not be very different if the ideal gas term is added. In the case of bosons there might appear a minimum at short distances due to the large ideal gas contribution near the origin.

The asymptotic behaviors of the correlation functions of fermions (Fig. 4) and bosons (Fig. 7) are somewhat similar. However, in the case of fermions the maximum is determined by the Fermi momentum which is density-dependent. In the case of bosons the general behavior of the correlation function does not change if the density is varied although the magnitude changes. In both cases the maxima are due to quantum effects and appear at relatively large reduced distances. For smaller x variables of orders of magnitude 1, exponential decays with certain decay constants characterize the correlation. Indeed, in the case of fermions we have

$$\frac{\Delta\rho_2(r)}{n^2}-1=-\frac{p_0^4}{8\pi^3 a_0 n^2}\left(1+\frac{1}{3\pi p_0 a_0}\right)\frac{e^{-\mu r}}{r}, \qquad (5.1)$$

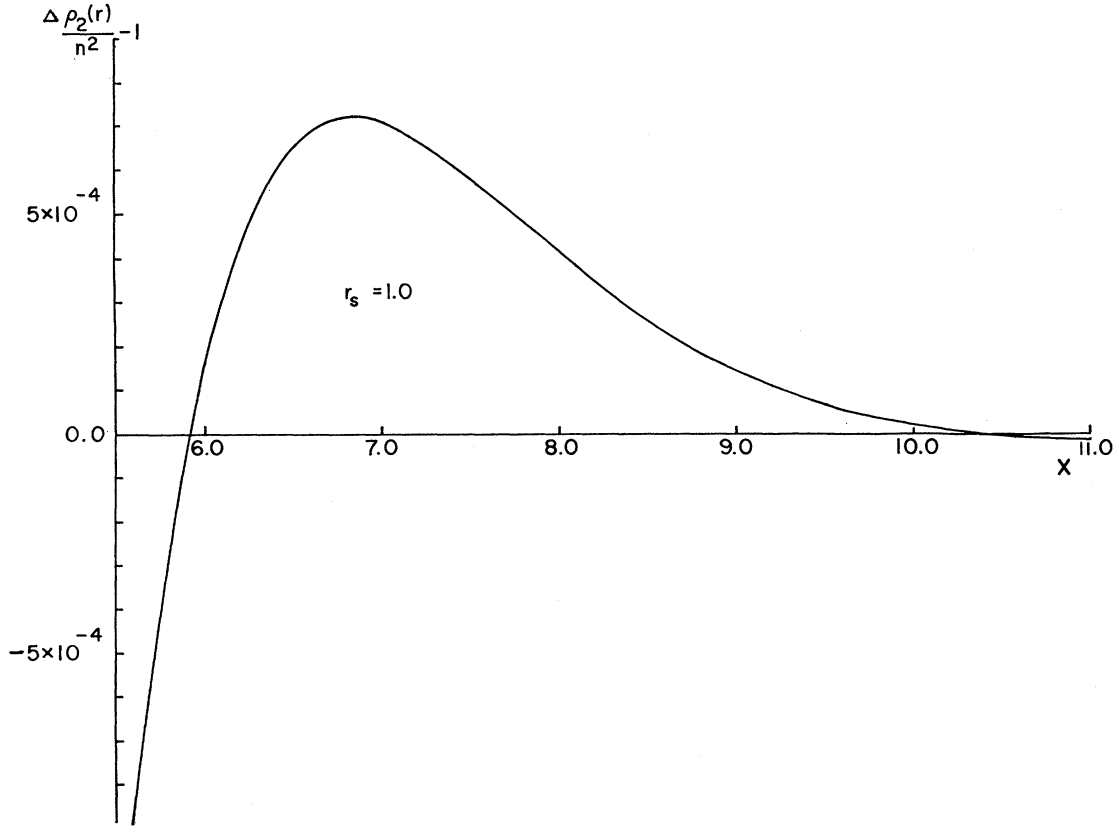

FIG. 7. Curve $r_s=1.0$ in Fig. 5 in a large scale.

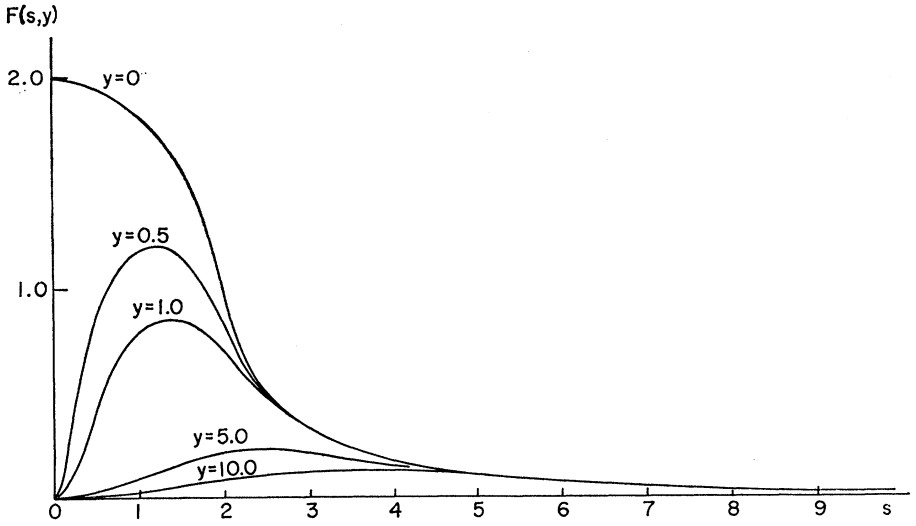

FIG. 8. Function $F(s,y)$ in the integrand of Eq. (3.2). The curve $y=0$ represents $F(s,0)$ defined in Eq. (5.4).

where

$$\mu=\mu_0\left(1+\frac{1}{6p_0a_0}\right). \tag{5.2}$$

Equation (5.1) corresponds to Eq. (4.3) for bosons. The same situation is observed in classical electron gases where the screening is effective at distances of order κ^{-1}.

As we have remarked in Sec. 3, our results improve upon the results based on the RPA. Indeed, if we pick up only $y=0$ term in Eq. (3.1) we arrive at

$$\frac{\Delta\rho_2(r)}{n^2}-1=-\frac{3}{2\pi^2}\left(\frac{3}{2\pi}\right)^{1/3}\frac{r_s}{x}\times\int_0^\infty ds\,\frac{sF^2(s,0)\sin sx}{s^2+s_0^2F(s,0)}, \tag{5.3}$$

where

$$F(s,0)=1-\frac{1}{4}\left(s-\frac{4}{s}\right)\ln\left|\frac{s+2}{s-2}\right|, \tag{5.4}$$

which has been used elsewhere. To illustrate the contribution of $y\neq0$ terms we have evaluated numerically the function $F(s,y)$. The results are shown in Fig. 8. The contribution from $y=0$ is certainly most important, but other terms also contribute. Note also the curves for $y\neq0$ do not have a maximum at $s=0$ but are zero. Because of this difference, it becomes not appropriate to expand the function $F(s,y)$ as Langer and Vosko did. Actually, there is no singularity of the function at $s=2$ if $y\neq0$. Thus, and because of the observation in Sec. 3, we conclude that the oscillating correlations should not be stressed for fermions at metallic densities.